Critical intra- and inter-sub-band plasmons in a Fibonacci HgTe/CdTe superlattice

1989 J. Phys.: Condens. Matter 1 4473

(http://iopscience.iop.org/0953-8984/1/27/022)

J. Phys.: Condens. Matter 1 (1989) 4473–4478. Printed in the UK

LETTER TO THE EDITOR

Critical intra- and inter-sub-band plasmons in a Fibonacci HgTe/CdTe superlattice

Danhong Huang†‡, Jianping Peng† and Shixun Zhou†
† Department of Physics, Fudan University, Shanghai, People's Republic of China
‡ China Center of Advanced Science and Technology (World Laboratory), PO Box 8730, Beijing, People's Republic of China

Received 30 March 1989

Abstract. We propose an equivalent transfer-matrix theory using the formal structure factors to study the critical plasmons in a Fibonacci HgTe/CdTe superlattice. In such a system, the bulk- and the surface-plasmon spectra will exhibit many different features when the surface layer of the semi-infinite superlattice is selected at different positions. It provides useful information about the surface-plasmon branch we are interested in for surface-wave device applications.

There has been a great deal of recent theoretical interest in the properties of layered electron gas (LEG) [1] and one-dimensional (1D) [2, 3] quasiperiodic systems. These systems show critical states in a manner similar to what is found for electrons. Critical states exist exactly at the mobility edge. A more significant development for Fibonacci systems is the recent fabrication [4] by Merlin and co-workers. On the other hand, Huang and Zhou [5, 6] have proposed the theory of collective excitations in HgTe/CdTe superlattice.

Conspicuous by its absence, however, is a calculation of intra- and inter-sub-band plasmons associated with the interface states in a Fibonacci HgTe/CdTe superlattice and inter-sub-band plasmons in general type-I and type-II Fibonacci superlattices. The aim of this Letter is to give the calculation of plasmon excitations in the semi-infinite Fibonacci HgTe/CdTe superlattice, where a rich spectrum may be expected.

The model system, along with the SCF theory, has been completely discussed by Huang and Zhou [5, 6], and we would like to omit any similar discussion about the model system in this Letter.

Let us consider F_m mini-cells, shown in figure 1(*a*), where F_m is a Fibonacci number, i.e., F_m satisfies a recursion relation $F_{m+1} = F_m + F_{m-1}$, with $F_0 = 1$, and $F_1 = 1$. The widths of mini-cell (A) and mini-cell (B) are chosen as d_A and d_B, respectively. In the *m*th generation there are F_m elements of the string [1]. This includes F_{m-1} mini-cells (A) and F_{m-2} mini-cells (B), e.g., the second generation produces the string A–B, and the third generation gives the string A–B–A. The ratio of the number of mini-cells (A) to the number of mini-cells (B) approaches the 'golden mean' value $\tau = (1 + 5^{1/2})/2$. The unit cell of the superlattice is then composed of F_m elements of the string. In contrast with the general Fibonacci model [1], in which the bulk plasmon spectrum remains unchanged, although the surface-plasmon spectrum may exhibit many different fea-

0953-8984/89/274473 + 06 $02.50

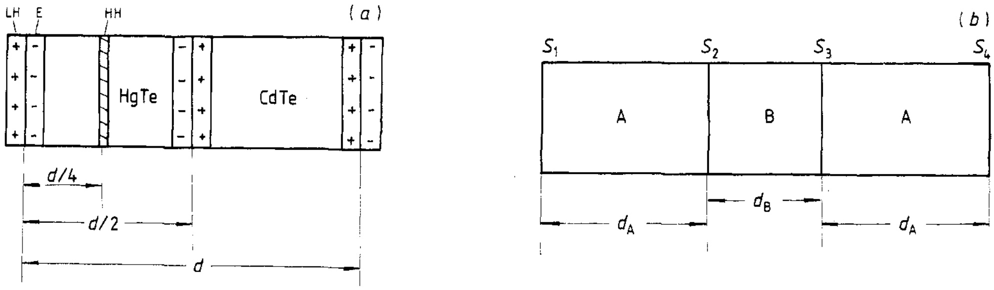

Figure 1. (*a*) The mini-cell of the HgTe/CdTe superlattice. The symbols E, LH, and HH stand for the electron, light-hole and heavy-hole layer, respectively. (*b*) The unit-cell of the Fibonacci HgTe/CdTe superlattice, in which the Fibonacci number F_m is chosen as $F_3 = 3$. d_A and d_B are the width of the mini-cell (A) and mini-cell (B), respectively.

tures, the mini-cell introduced here will produce three different features of the bulk plasmon spectra.

Considering the existence of the distribution of wavefunctions associated with interface states and bound heavy-hole-like states within a quantum well, we generalise the simplified transfer matrix given by Hawrylak and co-workers [1] referred to the ideal charged layer by introducing the formal structure factors S_E, S_{LH} and S_{HH} for electron-like, light-hole-like and heavy-hole-like states, respectively. Thus the charged interface and slab within the quantum well can be equivalently regarded as an 'ideal' charged layer again. Without repeated the lengthy derivation similar to that of [1], we directly write down the equivalent transfer matrices for mini-cell (A) and mini-cell (B), respectively

$$\mathbf{T}_A = \mathbf{T}_{LH}(d_A/4)\mathbf{T}_{HH}(d_A/4)\mathbf{T}_E(d_A/2) \tag{1}$$

$$\mathbf{T}_B = \mathbf{T}_{LH}(d_B/4)\mathbf{T}_{HH}(d_B/4)\mathbf{T}_E(d_B/2) \tag{2}$$

with $\mathbf{T}_E$, $\mathbf{T}_{LH}$ and $\mathbf{T}_{HH}$ given by

$$\mathbf{T}_E(d/2) = \begin{bmatrix} (1 + S_E^{-1}(d)) \exp(-qd/2) & S_E^{-1}(d) \exp(qd/2) \\ -S_E^{-1}(d) \exp(-qd/2) & (1 - S_E^{-1}(d)) \exp(qd/2) \end{bmatrix} \tag{3}$$

$$\mathbf{T}_{LH}(d/4) = \begin{bmatrix} (1 + S_{LH}^{-1}(d)) \exp(-qd/4) & S_{LH}^{-1}(d) \exp(qd/4) \\ -S_{LH}^{-1}(d)) \exp(-qd/4) & (1 - S_{LH}^{-1}(d)) \exp(qd/4) \end{bmatrix} \tag{4}$$

$$\mathbf{T}_{HH}(d/4) = \begin{bmatrix} (1 + S_{HH}^{-1}(d)) \exp(-qd/4) & S_{HH}^{-1}(d) \exp(qd/4) \\ -S_{HH}^{-1}(d) \exp(-qd/4) & (1 - S_{HH}^{-1}(d)) \exp(qd/4) \end{bmatrix} \tag{5}$$

where the formal structure factors $\mathbf{T}_E$, $\mathbf{T}_{LH}$ and $\mathbf{T}_{HH}$ are the relevant variables. The matrices $\mathbf{T}_E$, $\mathbf{T}_{LH}$, $\mathbf{T}_{HH}$, $\mathbf{T}_A$ and $\mathbf{T}_B$ are (2×2) matrices with a unit determinant. Note that the string of matrices $\{\mathbf{T}_{A(B)}\}$ is a Fibonacci sequence of matrices of $\mathbf{T}_A$ and $\mathbf{T}_B$ $\{\ldots\ldots \mathbf{T}_A\mathbf{T}_B\mathbf{T}_A\mathbf{T}_B\mathbf{T}_A\mathbf{T}_A\mathbf{T}_B\mathbf{T}_A\}$. Equations (1) and (2) are conveniently studied by the rational approximation method. A rational approximation m to a Fibonacci sequence consists of a periodic sequence of unit cells containing F_m matrices $\mathbf{T}_A$ and $\mathbf{T}_B$ corresponding to the different mini-cells (A) and (B) in the mth generation of the Fibonacci sequence. The bands consist of those values of the formal structure factors S_E, S_{LH} and

$S_{\rm HH}$ for which the trace of the equivalent transfer matrix across the unit cell is between -2 and $+2$. For the sake of comparison with the results given by the SCF theory [5, 6], we let $m = 1$, corresponding to the periodic HgTe/CdTe superlattice, and neglect the contribution of the heavy-hole-like states for the time being, then we get

$$\mathbf{T}_d = \mathbf{T}_{\rm LH}(d/2)\mathbf{T}_{\rm E}(d/2). \tag{6}$$

The rational approximation will give

$$1 - (S_{\rm E}^{-1} + S_{\rm LH}^{-1}\, S + S_{\rm E}^{-1}\, S_{\rm LH}^{-1} - 1(S^2 - S'^2) = 0 \tag{7}$$

where S and S' are the screening functions defined by

$$S = \sinh(qd)/[\cosh(qd) - \cos(q_z d)] \tag{8}$$

$$S' = 2\sinh(qd/2)\cos(q_z d/2)/[\cosh(qd) - \cos(q_z d)]. \tag{9}$$

On the other hand, the SCF theory [5, 6] gives

$$1-(\chi_{\rm E}+\chi_{\rm LH})[B-2\chi_{\rm E}\chi_{\rm LH}B(A-B)/(\chi_{\rm E}+\chi_{\rm LH})]S+\chi_{\rm E}\chi_{\rm LH}(S^2-S'^2)B^2$$
$$-(A-B)[(\chi_{\rm E}+\chi_{\rm LH})-\chi_{\rm E}\chi_{\rm LH}(A-B)]=0 \tag{10}$$

where $\chi_{\rm E}$ and $\chi_{\rm LH}$ stand for the susceptibilities of the electron and the light hole, respectively, and the symbols A, B are defined as the screened Coulomb interaction [5, 6], which will be explicitly written out below. Comparing (7) with (10), we can easily obtain

$$S_{\rm E}^{-1} = \chi_{\rm E}B/[1 - \chi_{\rm E}(A - B)] \tag{11}$$

$$S_{\rm LH}^{-1} = \chi_{\rm LH}B/[1 - \chi_{\rm LH}(A - B)]. \tag{12}$$

From (11) and (12) we easily know that

$$S_{\rm HH}^{-1} = \chi_{\rm HH}G/[1 - \chi_{\rm HH}(V - G)] \tag{13}$$

where the symbols V and G are similar to A and B, and will also be explicitly written out below. It is really quite an intuitive result, i.e., if we replace $S_{\rm HH}$ in (13) by S in (8), then we can obtain the collective excitation spectrum in a general type-I superlattice.

For the intra-sub-band mode, we have [5, 6]

$$\chi_{\rm E}(\boldsymbol{q},\omega) = n_{\rm E}q^2/m_{\rm E}\omega^2(2\pi e^2/\varepsilon_{\rm s}q) \tag{14a}$$

$$\chi_{\rm LH}(\boldsymbol{q},\omega) = n_{\rm LH}q^2/m_{\rm LH}\omega^2(2\pi e^2/\varepsilon_{\rm s}q) \tag{14b}$$

$$\chi_{\rm HH}(\boldsymbol{q},\omega) = n_{\rm HH}q^2/m_{\rm HH}\omega^2(2\pi e^2/\varepsilon_{s}q) \tag{14c}$$

and

$$A=\{4[2+\exp(-\beta d/2)]/[d+2\sinh(\beta d/2)/\beta]^2\}[\![2q/(q^2-4\beta^2)$$
$$\times[\sinh(\beta d/2)/\beta+\sinh(\beta d)/4\beta+d/4]+[d+2\sinh(\beta d/2)/\beta]/q$$
$$-\{\exp[-(2\beta+q)d/4]/(2\beta+q)-\exp[(2\beta-q)d/4]/(2\beta-q)$$
$$+2\exp(-qd/4)/q\}\sinh[(2\beta+q)d/4]/(2\beta+q)$$
$$+\sinh[(2\beta-q)d/4]/(2\beta-q)+2\sinh(qd/4)/q\}]\!] \tag{15a}$$

$$B=\{4[2+\exp(-\beta d/2)]/[d+2\sinh(\beta d/2)/\beta]^2\}\{\sinh[(2\beta+q)d/4]/(2\beta+q)$$
$$+\sinh[(2\beta-q)d/4]/(2\beta-q)+2\sinh(qd/4)/q\}^2 \qquad (15b)$$
$$V=G=1. \qquad (15c)$$

Here we have introduced the δ-function approximation [5] in (15*c*).

For the inter-sub-band mode, on the other hand, we have [5, 6]

$$\chi_{\rm E}(\boldsymbol{q},\omega)=2n_{\rm E}\Omega_{10}/\hbar(\omega^2-\Omega_{10}^2)(2\pi e^2/\varepsilon_s q) \qquad (16a)$$
$$\chi_{\rm LH}(\boldsymbol{q},\omega)=[2n_{\rm LH}\Omega_{10}/\hbar(\omega^2-\Omega_{10}^2)](2\pi e^2/\varepsilon_s q) \qquad (16b)$$
$$\chi_{\rm HH}(\boldsymbol{q},\omega)=[2n_{\rm HH}\Omega_{10}^*/\hbar(\omega^2-\Omega_{10}^{*2})](2\pi e^2/\varepsilon_s q) \qquad (16c)$$

and

$$A=\{8/[4\sinh^2(\beta d/2)/\beta^2-d^2)\}[\![q[\sinh(\beta d)-\beta d]/[2\beta(q^2-4\beta^2)]$$
$$+\{\exp[-(2\beta+q)d/4]/(2\beta+q)+\exp[(2\beta-q)d/4]/(2\beta-q)\}$$
$$\times\{\sinh[(2\beta+q)d/4]/(2\beta+q)-\sinh[(2\beta-q)d/4]/(2\beta-q)\}]\!] \qquad (17a)$$
$$B=\{-8/[4\sinh^2(\beta d/2)/\beta^2-d^2]\}\{\sinh[(2\beta-q)d/4]/(2\beta-q)$$
$$-\sinh(2\beta+q)d/4]/(2\beta+q)\}^2 \qquad (17b)$$
$$V=(qd/2)\{1/[(qd/2)^2+\pi^2]+1/[(qd/2)^2+9\pi^2]\}$$
$$-(qd)^2\cosh(qd/4)\exp(-qd/4)\{1/[(qd/2)^2+\pi^2]$$
$$-1/[(qd/2)^2+9\pi]\}^2 \qquad (17c)$$
$$G=-(qd)^2\cosh^2(qd/4)\{1/[(qd/2)^2+\pi^2]-1/[(qd/2)^2+9\pi^2]\}^2 \qquad (17d)$$

where we have assumed $L_{\rm HH}=d/2$ in (17*d*) for convenience.

Following [1], we define the (2×2) matrix $\mathbf{M}_m$ as $\mathbf{M}_m=\Pi_{i=1}^{F_m}\mathbf{T}_i$, where $\mathbf{T}_i$ is a matrix $\mathbf{T}_A$ or $\mathbf{T}_B$ in Fibonacci sequence, and $X_m=\mathrm{Tr}(\mathbf{M}_m)/2$, then the bulk plasmon mode in Fibonacci HgTe/CdTe superlattice can be written as [1]

$$X_m=\mathrm{Tr}(\mathbf{M}_m)/2=\cos(q_z D_m) \qquad (18)$$

where D_m is the length of unit cell composed of F_m elements of the string. Furthermore, if we use the boundary condition for the electric potential at the surface layer, then the surface-plasmon mode is given by

$$(\varepsilon_s+\varepsilon_0-2\varepsilon_s S_x^{-1})]/[\varepsilon_s-\varepsilon_0+2\varepsilon_s S_x^{-1})+[(M_m)_{11}\pm\exp(-\kappa D_m)]/(M_m)_{12}=0 \qquad (19)$$

where

$$\kappa D_m=\ln[|\mathrm{X}_m|+(|\mathrm{X}_m|^2-1)^{1/2}] \qquad (20)$$

and S_x^{-1} stands for the formal structure factor referred to the different state in the surface layer, i.e., $S_{\rm E}^{-1}$, $S_{\rm LH}^{-1}$ or $S_{\rm HH}^{-1}$.

We now turn to the plasmon spectrum obtained using (18) and (19). For the sake of convenience, we only give, as an example, the intra-sub-band-plasmon mode in both the periodic superlattice and the Fibonacci superlattice for comparison. It is evident that the inter-sub-band-plasmon mode can be given in a similar way, and there will be no fundamental difficulty in calculating its spectrum. Moreover, we let $m=3$ here to simplify the calculation. The unit cell composed of three elements of the string is shown

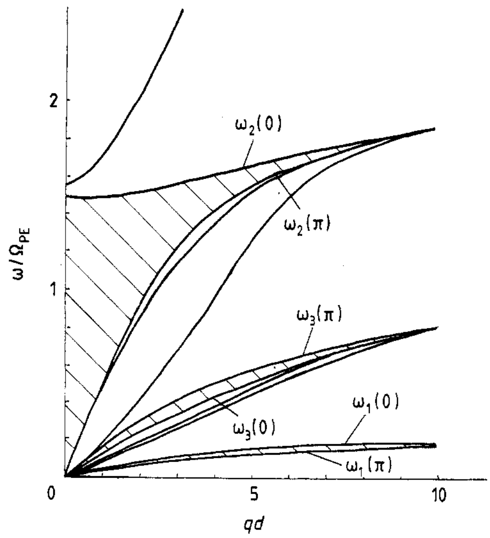

Figure 2. The plasmon spectrum of the periodic HgTe/CdTe superlattice. The parameters are chosen as $(\Omega_{HH}/\Omega_{PE})^2 = \frac{1}{5}$, $(\Omega_{PH}/\Omega_{PE})^2 = 1/55$ and $\beta d = 7.742$. The symbols Ω_{PE}, Ω_{PH} and Ω_{HH} are the three-dimensional plasmon frequencies of the electron, light hole and heavy hole, respectively. β^{-1} is the localisation length of the interface state.

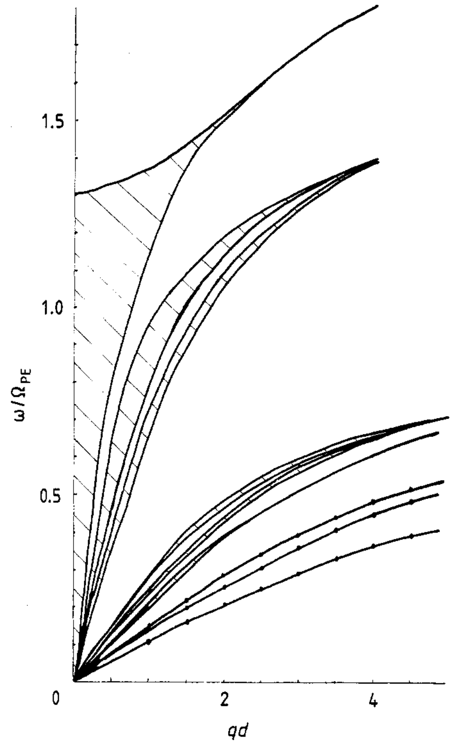

Figure 3. The plasmon spectrum of the Fibonacci HgTe/CdTe superlattice. The parameters are chosen as $(\Omega_{HH}/\Omega_{PE})^2 = \frac{1}{5}$, $(\Omega_{PH}/\Omega_{PE})^2 = \frac{1}{10}$, $(d_A/d_B) = 1.618$ and $\beta d_B = 0.7742$. The symbols Ω_{PE}, Ω_{PH}, Ω_{HH} and β^{-1} have the same meaning as in figure 2.

in figure 1(*b*). Figure 2 presents the intra-sub-band-plasmon spectrum in the periodic HgTe/CdTe superlattice. From it we find that the optical-plasmon mode associated with the heavy-hole-like state is suppressed, due to the Coulomb interaction between the interface states and the bound heavy-hole-like states within the same quantum well. In addition, we also find several attractive surface-plasmon branches that degenerate with two different bulk-plasmon bands in the weak-screening and strong-screening regions, respectively, in comparison with those in type-I and type II superlattices. In figure 3, the intra-sub-band-plasmon spectrum in the Fibonacci HgTe/CdTe superlattice is shown, in which the ' golden mean' ratio $d_A/d_B = 1.618$ is chosen. From it we find that each bulk-plasmon branch is split into three ($F_3 = 3$) branches in comparison with those in figure 2. Here we do not show the surface-plasmon branches, since some of them are too close to the bulk-plasmon bands to be clearly indicated. We should emphasise [1] that as $M \rightarrow \infty$ we will see an infinite number of very narrow bands that have a typical self-similar Cantor-set structure. From the theoretical analysis, we easily know that there are three different kinds of mini-cells, corresponding to the first charged layer in figure 1(*a*) being selected as the electron, light-hole, or heavy-hole layer, respectively. This leads to the three different features of the bulk plasmon spectra. On the other hand, there are F_m different kinds of unit cells composed of F_m elements of the string for a given mini-cell, corresponding to the first layer being selected at $S_1, S_2, S_3, S_4, \ldots, S_m$, respectively. This leads to the different features of the surface-plasmon spectra, while the bulk-plasmon spectrum remains the same.

From the discussions above, we know that, in general, there will be three different features of the bulk-plasmon spectra and, for each given bulk plasmon spectrum, there still exist F_m different features of the surface-plasmon spectrum; thus we will in total get $3F_m$ different features of the surface-plasmon spectra in such a Fibonacci system.

In conclusion, the equivalent transfer-matrix theory has taken into account the distribution of wavefunctions within the quantum well, and can also be used to calculate the inter-sub-band-plasmon modes in general Fibonacci type-I and type-II superlattices. We expect that this will provide us with useful information about the selection of the surface-plasmon branch we are interested in for surface-wave device applications.

This work was supported in part by the Chinese Science Foundation through Grant No-1860723 and No-8688708, and in part by the Chinese Higher Education Foundation through Grant No 2-1987.

References

[1] Hawrylak P, Eliasson G and Quinn J J 1987 *Phys. Rev.* B **36** 6501
[2] Sarma S D, Kobayashi A and Prange R E 1986 *Phys. Rev. Lett.* **56** 1280; *Phys. Rev.* B **34** 5309
[3] Hawrylak P and Quinn J J 1986 *Phys. Rev. Lett.* **57** 380
[4] Merlin R, Bajema K, Clarke R, Juang F Y and Bhattacharya P K 1985 *Phys. Rev. Lett.* **55** 1768
Todd J, Merlin R, Clarke R, Mohanty K M and Axe J D 1986 *Phys. Rev. Lett.* **57** 1157
[5] Danhong Huang and Shixun Zhou 1988 *Phys. Rev.* B **38** 13061
[6] Danhong Huang and Shixun Zhou 1988 *Phys. Rev.* B **38** 13069